NUMERICAL SIMULATIONS OF VISCOELASTIC FLUID FLOWS IN A PLANAR *CROSS-SLOT* GEOMETRY

Dário Canossi, dario.oliveira@etudiant.univ-lille1.fr[1]
Ramon Martins, ramon.martins@polytech-lille.fr[1]
Gilmar Mompean, gilmar.mompean@polytech-lille.fr[1]

[1]Laboratoire de Mécanique de Lille (LML), CNRS/FRE 3723, Polytech'Lille.
Université des Sciences et Technologies de Lille, Cité Scientifique, Villeneuve d'Ascq, 59655, France.

Abstract: *In this work, a square-root formulation is implemented in a finite-volume numerical code and used to simulate the flow of an Oldroyd-B viscoelastic fluid in a channel and a planar* cross-slot *geometries. These results are validated by comparing them to previous numerical results, obtained using a standard extra-stress tensor formulation and also to analytic solution, in order to exhibit the benefits of the square-root formulation for the studied geometries.*
Keywords: *viscoelasticity, simulation, cross-slot*

1. INTRODUCTION

Existing models of viscoelastic fluids present challenging problems for numerical computation, since the direct calculation of the viscoelastic extra-stress tensor evolution produces numerical instabilities that lead to the loss of positive-definiteness of the conformation tensor, what causes the numerical scheme to break down (Dupret and Marchal, 1986).

In this context, Sureshkumar and Beris (1995) firstly overcame this issue by adding an artificial stress diffusion term into the numerical problem. However, even if this solution is largely used, it brings a non-physical term into the equation, which must be adjusted to be as small as possible. One year later, Sun *et al.* (1996) presented results for an adaptive version of a viscoelastic stress splitting scheme, which has been named *AVSS scheme* and performed very well for higher Weissenberg values of viscoelastic flows. The merits of each one of these strategies to stabilize the numerical computation of non-Newtonian fluids have been systematically studied later (Amoreira and Oliveira, 2010).

Following to the *AVSS scheme*, other remarkable methodologies have been introduced, as, for instance, the log-conformation (Fattal and Kupferman, 2004), the square-root (Balci *et al.*, 2011) and the kernel (Afonso *et al.*, 2012) transformations. These promising methods have been applied to (very) low Reynolds number cases and high Weissenberg numbers in 2D or three-periodic cases, with good results.

In the present work, we apply the square-root formulation (Balci *et al.*, 2011) to Oldroyd-B fluid for a channel and a *cross-slot* laminar flows. Such results are compared with those obtained from the standard formulation by Mompean and Deville (1997). Potential benefits of this formulation are also discussed.

2. NUMERICAL METHOD

In the present study, the flow of an isothermal, incompressible, viscoelastic fluid flow is considered. Under these conditions, the set of equations that needs to be solved is the conservation of mass,

$$\nabla \cdot \mathbf{u} = 0\,, \tag{1}$$

along with the momentum conservation equation,

$$\rho\left[\frac{\partial \mathbf{u}}{\partial t} + \nabla \cdot (\mathbf{uu})\right] = -\nabla p + \nabla \cdot (\eta_0 \nabla \mathbf{u} + \mathbf{T}) + \rho \mathbf{g}\,, \tag{2}$$

where $\mathbf{u}$ represents the velocity vector, $\mathbf{T}$ the viscoelastic extra-stress tensor, p the pressure, ρ the volumetric mass density, η_0 the zero-shear viscosity and $\mathbf{g}$ the gravity.

The numerical method used to solve the above equations is a finite-volume technique in space and second-order discretization in time (Adams-Bashforth two-step method), whereas a semi-implicit code is used for the numerical calculations. A detailed description of this code formulation is presented in the work of Mompean and Deville (1997).

2.1 Extra-stress evolution

The tensor $\mathbf{T}$ that figures in Eq. (2) can be described in many different ways, depending on the viscoelastic model chosen. The Oldroyd-B model is an extension of the Upper Convected Maxwell model and presents a constitutive equation capable of describing the viscoelastic behaviour of non-Newtonian polymeric solutions under general flow conditions. The constitutive equation for the viscoelastic extra-stress tensor $\mathbf{T}$, according to the Oldroyd-B model, is (Bird *et al.*, 1987):

$$\mathbf{T} + \lambda\left[\frac{\partial \mathbf{T}}{\partial t} + \nabla \cdot (\mathbf{uT}) - (\nabla \mathbf{u})^T \cdot \mathbf{T} - \mathbf{T} \cdot \nabla \mathbf{u}\right] = \eta_1 \dot{\gamma}\,, \tag{3}$$

where the superscript T denotes the transpose matrix, λ is the material relaxation time, η_1 is the constant polymeric viscosity and $\dot{\gamma}$ is the rate-of-strain tensor, defined as $\dot{\gamma} = \nabla\mathbf{u} + (\nabla\mathbf{u})^T$.

2.1.1 *Conformation tensor formulation*

The Oldroyd-B model can also describe polymer molecules orientation by making use of a conformation tensor, which is, by definition, symmetric positive-definite (SPD). The polymer conformation tensor $\mathbf{c}$ evolves according to the equation:

$$\frac{D\mathbf{c}}{Dt} = \mathbf{c}\cdot\nabla\mathbf{u} + \nabla\mathbf{u}^T\cdot\mathbf{c} + \mathbf{s}(\mathbf{c})\,, \tag{4}$$

where the quantity $\dfrac{D}{Dt}$ represents a *material derivative*.

The tensor $\mathbf{s}(\mathbf{c})$ in Eq. (4) takes different forms, depending on the non-Newtonian model assumed. For the Oldroyd-B model, we have:

$$\mathbf{s}(\mathbf{c}) = \frac{1}{Wi_b}(\mathbf{I}-\mathbf{c})\,. \tag{5}$$

Wi_b is the Weissenberg number, defined as:

$$Wi_b = \frac{U\lambda}{l}\,, \tag{6}$$

where U is the inlet bulk velocity and l is a characteristic length.

It is important to remark that the velocity gradient tensor has entries $\nabla u_{ij} = \partial u_j/\partial x_i$.

2.1.2 *Square-root formulation*

Balci *et al.* (2011) proposed the square-root transformation for the conformation tensor $\mathbf{c}$. The square-root (matrix) of the conformation tensor $\mathbf{b}$ is considered and the conformation tensor may be recovered by the following operation:

$$\mathbf{c} = \mathbf{b}^T\cdot\mathbf{b}\,. \tag{7}$$

The square-root tensor $\mathbf{b}$ being symmetric, Eq. (7) also writes $\mathbf{c} = \mathbf{b}\cdot\mathbf{b}$.

Replacing Eq. (7) into Eq. (4), using Eq. (5), yields

$$\frac{D\mathbf{b}^T}{Dt}\cdot\mathbf{b} + \mathbf{b}^T\cdot\frac{D\mathbf{b}}{Dt} - \mathbf{b}^T\cdot\mathbf{b}\cdot\nabla\mathbf{u} - \nabla\mathbf{u}^T\cdot\mathbf{b}^T\cdot\mathbf{b} + \frac{\mathbf{b}^T\cdot\mathbf{b}-\mathbf{I}}{Wi_b} = 0\,. \tag{8}$$

Multiplying Eq. (8) on the left by $\mathbf{b}^{-T}$ and on the right by $\mathbf{b}^{-1}$, and rearranging, yields

$$\left(\frac{D\mathbf{b}}{Dt} - \mathbf{b}\cdot\nabla\mathbf{u} + \frac{\mathbf{b}-\mathbf{b}^{-T}}{2Wi_b}\right)\cdot\mathbf{b}^{-1} = -\mathbf{b}^{-T}\cdot\left(\frac{D\mathbf{b}^T}{Dt} - \nabla\mathbf{u}^T\cdot\mathbf{b}^T + \frac{\mathbf{b}^T-\mathbf{b}^{-1}}{2Wi_b}\right)\,. \tag{9}$$

Regarding Eq. (9), it is easily shown that one side is minus the transpose of the other. Therefore, each side of this equation must be anti-symmetric, yielding

$$\left(\frac{D\mathbf{b}}{Dt} - \mathbf{b}\cdot\nabla\mathbf{u} + \frac{\mathbf{b}-\mathbf{b}^{-T}}{2Wi_b}\right)\cdot\mathbf{b}^{-1} = \mathbf{a}\,, \tag{10}$$

or

$$-\mathbf{b}^{-T}\cdot\left(\frac{D\mathbf{b}^T}{Dt} - \nabla\mathbf{u}^T\cdot\mathbf{b}^T + \frac{\mathbf{b}^T-\mathbf{b}^{-1}}{2Wi_b}\right) = \mathbf{a}\,, \tag{11}$$

where $\mathbf{a}$ is an anti-symmetric tensor. Since $\mathbf{b} = \mathbf{b}^T$ and the goal here is to find an evolution equation for the square-root of the conformation tensor, one can either multiply Eq. (10) on the left by $\mathbf{b}$ or Eq. (11) on the right by $\mathbf{b}^T$, which respectively gives

$$\frac{D\mathbf{b}}{Dt} - \mathbf{b}\cdot\nabla\mathbf{u} - \mathbf{a}\cdot\mathbf{b} + \frac{\mathbf{b}-\mathbf{b}^{-1}}{2Wi_b} = 0\,, \tag{12}$$

and

$$\frac{D\mathbf{b}}{Dt} - \nabla\mathbf{u}^T\cdot\mathbf{b} + \mathbf{b}\cdot\mathbf{a} + \frac{\mathbf{b}-\mathbf{b}^{-1}}{2Wi_b} = 0\,. \tag{13}$$

In both Eqs. (12) and (13), the first and the last terms on the left-hand side are symmetric. Defining $\mathbf{r} = \mathbf{b}\cdot\nabla\mathbf{u} + \mathbf{a}\cdot\mathbf{b}$, the transpose of $\mathbf{r}$ is $\mathbf{r}^T = \nabla\mathbf{u}^T\cdot\mathbf{b}^T + \mathbf{b}^T\cdot\mathbf{a}^T = \nabla\mathbf{u}^T\cdot\mathbf{b} - \mathbf{b}\cdot\mathbf{a}$. It is important to remark that the non-symmetric terms in Eq. (12) are equal to $-\mathbf{r}$ and, in Eq. (13), equal to $-\mathbf{r}^T$. Since Eq. (12) is equal to Eq. (13), $\mathbf{r}$ must be equal to $\mathbf{r}^T$, which implies that $\mathbf{r}$ is symmetric. Thus, if $\mathbf{r} = \mathbf{r}^T$, the entries of $\mathbf{a}$ can be calculated as a function of $\mathbf{b}$ and $\nabla\mathbf{u}$ by the relation $r_{ij} = r_{ji}$, which yields the linear system

$$\begin{pmatrix} b_{11}+b_{22} & b_{23} & -b_{13} \\ b_{23} & b_{11}+b_{33} & b_{12} \\ -b_{13} & b_{12} & b_{22}+b_{33} \end{pmatrix} \begin{pmatrix} a_{12} \\ a_{13} \\ a_{23} \end{pmatrix} = \begin{pmatrix} t_1 \\ t_2 \\ t_3 \end{pmatrix}, \tag{14}$$

where the terms $t_{1,2,3}$ are given by

$$\begin{aligned} t_1 &= (b_{12}\nabla u_{11} - b_{11}\nabla u_{12}) + (b_{22}\nabla u_{21} - b_{12}\nabla u_{22}) + (b_{23}\nabla u_{31} - b_{13}\nabla u_{32}) \\ t_2 &= (b_{13}\nabla u_{11} - b_{11}\nabla u_{13}) + (b_{33}\nabla u_{31} - b_{13}\nabla u_{33}) + (b_{23}\nabla u_{21} - b_{12}\nabla u_{23}) \\ t_3 &= (b_{13}\nabla u_{12} - b_{12}\nabla u_{13}) + (b_{23}\nabla u_{22} - b_{22}\nabla u_{23}) + (b_{33}\nabla u_{32} - b_{23}\nabla u_{33}) \end{aligned} . \tag{15}$$

3. VALIDATION AND RESULTS

Simulations have been performed in two different geometries, a two-dimensional planar channel and the well-known *cross-slot* geometry. Both studied geometries are shown schematically in Fig. 1.

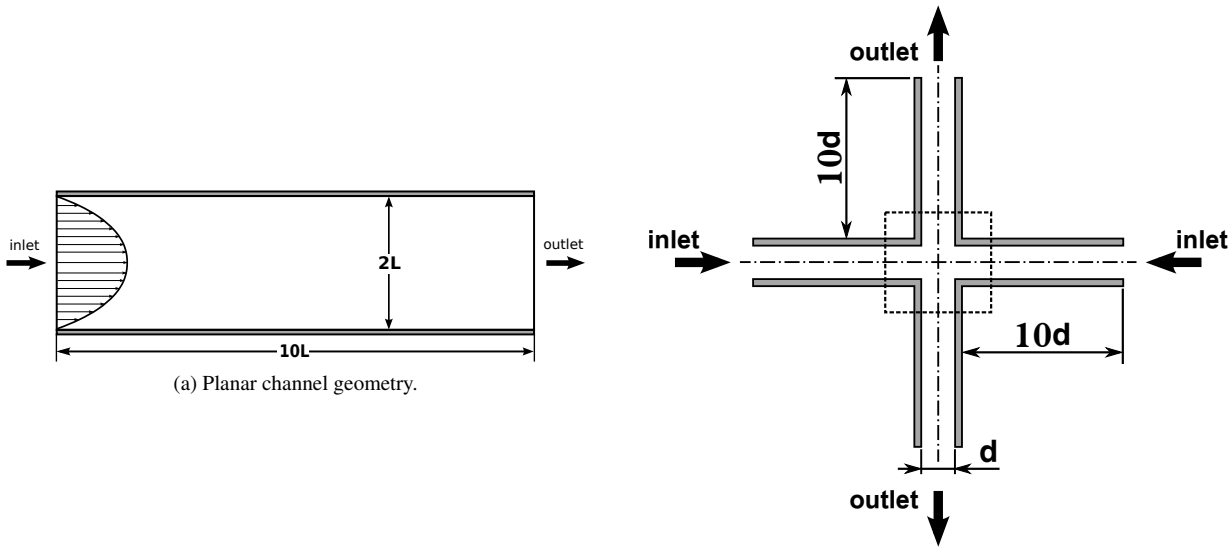

(a) Planar channel geometry.

(b) *Cross-slot* geometry.

Figure 1: Schematics of the geometries.

3.1 Planar channel

The channel length and width were fixed at a $10:2$ proportion to ensure a fully-developed flow away from the inlet. A regular quadrilateral mesh was used, with 100 x 50 cells. Fully-developed velocity profile (with average value $U = U_{in}$) is applied at the inlet and Dirichlet boundary condition for the pressure is assumed at the outlet. At the walls, we apply the no-slip and impenetrability conditions (i.e. $u = v = 0$). Table 1 summarizes the flow parameters for the channel simulations.

Table 1: **Simulation parameters for the channel flow.**

Symbol	Property $(unit)$	Value
L	Half-width (m)	1.0
ρ	Density (kg/m^3)	1.0
η_0	Zero-shear viscosity (Pl)	1.0
η_1	Polymeric viscosity (Pl)	8.0
λ	Relaxation time (s)	0.012
Re	Reynolds number	1.0
De	Deborah number	0.1

The fully-developed profiles for the extra-stress tensor and velocity components have been compared to the analytic solution, provided by Dallas *et al.* (2010), which is shown in Fig. 2 for a Reynolds (Re) and Deborah (De) number equal to 1.0 and 0.1, respectively, at the channel central plane.

Concerning the simulations performed following the square-root formulation, the extra-stress tensor $\mathbf{T}$ is retrieved from the square-root tensor $\mathbf{b}$ using the relation shown in Eq. 16,

$$\mathbf{T} = \frac{\eta_1}{\lambda} \left(\mathbf{b} \cdot \mathbf{b} - \mathbf{I} \right) . \tag{16}$$

The velocity profile exhibited in Fig. 2a is nondimensionalized by the bulk velocity U, while the extra-stress profiles in Figs. 2b, 2c and 2d are nondimensionalized according to Eq. 17,

$$T^* = T \, \frac{2L}{U \left(\eta_0 + \eta_1 \right)} . \tag{17}$$

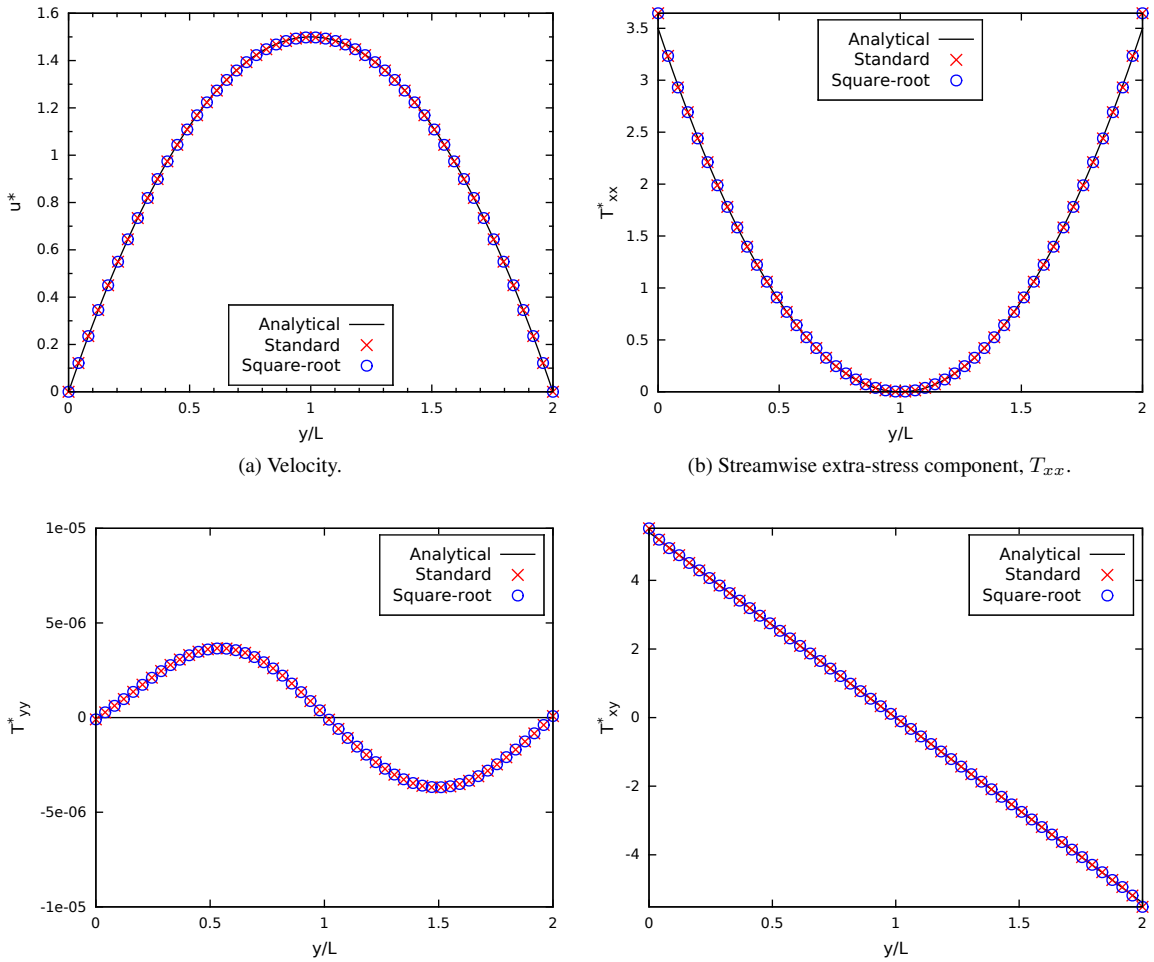

(a) Velocity.

(b) Streamwise extra-stress component, T_{xx}.

(c) Spanwise extra-stress component, T_{yy}.

(d) Shearwise extra-stress component, T_{xy}.

Figure 2: Dimensionless profiles at the middle of the channel.

An explicit result presented in Fig. 2 is the very good agreement between the two formulations (standard and square-root), for each one of the four profiles. These formulations are validated by a comparison to the analytic solution for the same profiles. One can notice that the difference found in Fig. 2c is due to numerical round-off errors.

Beyond that, simulations have been performed for several parameters variations - resulting in varied Reynolds and Deborah number flows - and same agreement between both formulations was found for all the components profiles, and also for evolution in time (not shown here).

3.2 Cross-slot

The *cross-slot* arrangement consists of two perpendicular and bisecting channels with two opposing inlets and outlets (see Fig. 1b), which results in a flow field with a stagnation point at the center of the geometry, where the flow velocity is zero. Flow is provided in each inlet arm of width d with bulk velocity U. At the symmetric central plane $x = 0$, the two inlet streams meet and proceed to the two outlet arms, of identical width d. The lengths of each one of the four arms are $10d$, which is confirmed to be enough for the flow to be fully developed (Poole *et al.*, 2014). For illustration, we see in Fig. 3 a snapshot of a converged low-elasticity flow simulation (Re = 0.01 and De = 0.01). The pressure contours are nondimensionalized according to Eq. 18,

$$p^* = p \, \frac{2}{U^2} . \tag{18}$$

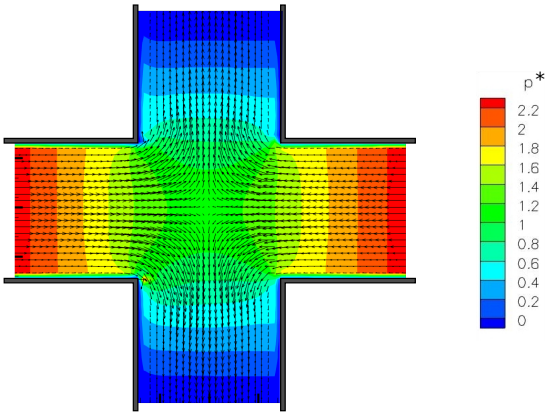

Figure 3: Velocity profiles (arrows) and pressure contours (colors) for a low-elasticity flow.

For both the standard and the square-root formulation, we use two meshes with a geometric progression for the element sizes in the four arms, with increased density closer to the center of symmetry. In the central square, there is an uniform mesh with cell spacing $\Delta x_{min} = \Delta y_{min}$. Mesh $M50$ has $\Delta x_{min} = 0.02\,d$ and mesh $M100$ has $\Delta x_{min} = 0.01d$. Similarly to the channel simulation, fully-developed velocity profile is applied at both inlets and zero pressure condition is assumed at the outlets. No-slip and impenetrability conditions are also considered. Table 2 displays the flow parameters for the *cross-slot* simulations.

Table 2: **Simulation parameters for the *cross-slot* flow.**

Symbol	Property $(unit)$	Value
d	Width (m)	0.01
ρ	Density (kg/m^3)	1000
η_0	Zero-shear viscosity (Pl)	0.005
η_1	Polymeric viscosity (Pl)	0.04
λ	Relaxation time (s)	20.0
Re	Reynolds number	0.01
De	Deborah number	0.1

Cruz *et al.* (2014) defined a benchmark variable Wi_0 for viscoelastic flow, calculated using the strain rate $\dot{\varepsilon}_0$ at the central stagnation point,

$$Wi_0 = \lambda\,\dot{\varepsilon}_0 = \lambda\sqrt{\left(\left.\frac{\partial u}{\partial x}\right|_0\right)^2 + \left.\frac{\partial u}{\partial y}\right|_0 \left.\frac{\partial v}{\partial x}\right|_0}\,. \tag{19}$$

The time evolution for this benchmark value appears in Fig. 4. With appropriate mesh refinement, this variable presents a good convergence to the literature estimation. Furthermore, we observe a nice agreement between the original extra-stress tensor and the square-root formulations.

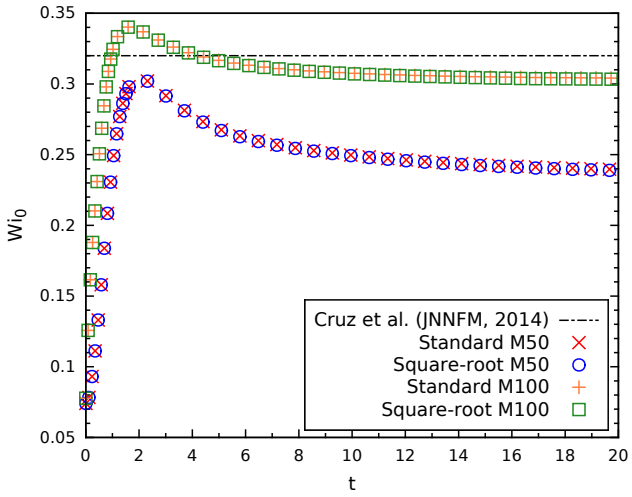

Figure 4: Time evolution for the local Weissenberg benchmark Wi_0, as defined by Eq. 19.

4. FINAL CONSIDERATIONS

These preliminary results aim to validate the implementation of the square-root formulation into this numerical code, for laminar flows with moderate viscoelasticity.

A simple and a rather complex geometry were studied, in order to access the coverage of the square-root method and its adaptability in geometries with stagnation points.

In a future work, we hope to extend our work to tridimensional geometries and moreover, determine whether this mathematical formulation proves itself as a powerful technique to increase numerical stability in a semi-implicit finite-volume code, enabling simulations at increasingly viscoelastic flows, at which the standard formulation fails.

5. ACKNOWLEDGEMENTS

This work was conducted with the support of CNPq (Brazilian National Council of Technological and Scientific Development), during a scholarship through its international cooperation program *Science Without Borders*. The authors would like to express their acknowledgements to the *Centre de Ressources Informatiques* (CRI) from *Université de Lille 1* for the use of its computational facilities.

6. REFERENCES

Afonso, A.M., Pinho, F.T. and Alves, M.A., 2012. "The *kernel*-conformation constintutive laws". *J Non-Newton Fluid*, Vol. 167-168, pp. 30–37.

Amoreira, L.J. and Oliveira, P.J., 2010. "Comparison of different formulations for the numerical calculation of unsteady incompressible viscoelastic fluid flow". *Adv. Appl. Math. Mech.*, Vol. 2, No. 4, pp. 483–502.

Balci, N., Thomases, B., Renardy, M. and Doering, C.R., 2011. "Symmetric factorization of the conformation tensor in viscoelastic fluid models". *J Non-Newton Fluid*, Vol. 166, pp. 546–553.

Bird, R.B., Armstrong, R.C. and Hassager, O., 1987. *Dynamics of Polymeric Liquids*. John Wiley & Sons, New York.

Cruz, F.A., Poole, R.J., Afonso, A.M., Pinho, F.T., Oliveira, P.J. and Alves, M.A., 2014. "A new viscoelastic benchmark flow: Stationary bifurcation in a cross-slot". *J Non-Newton Fluid*, Vol. 214, pp. 57–68.

Dallas, V., Vassilicos, J.C. and Hewitt, G.F., 2010. "Strong polymer-turbulence interactions in viscoelastic turbulent channel flow". *Physical Review E*, Vol. 82, pp. 066303–1–066303–19.

Dupret, F. and Marchal, J.M., 1986. "Loss of evolution in the flow of viscoelastic fluids". *J Non-Newton Fluid*, Vol. 20, pp. 143–171.

Fattal, R. and Kupferman, R., 2004. "Constitutive laws for the matrix-logarithm of the conformation tensor". *J Non-Newton Fluid*, Vol. 123, No. 2-3, pp. 281–285.

Mompean, G. and Deville, M., 1997. "Unsteady finite volume simulation of oldroyd-b fluid through a three-dimensional planar contraction". *J Non-Newton Fluid*, Vol. 72, pp. 253–279.

Poole, R.J., Rocha, G.N. and Oliveira, P.J., 2014. "A symmetry-breaking inertial bifurcation in a cross-slot flow". *Computers & Fluids*, Vol. 93, pp. 91–99.

Sun, J., Phan-Thien, N. and Tanner, R.I., 1996. "An adaptive viscoelastic stress splitting scheme and its applications: Avss/si and avss/supg". *J Non-Newton Fluid*, Vol. 65, pp. 75–91.

Sureshkumar, R. and Beris, A.N., 1995. "Effect of artificial stress diffusivity on the stability of numerical calculations and the dynamics of time-dependent viscoelastic flows". *J Non-Newton Fluid*, Vol. 60, pp. 53–80.

7. RESPONSIBILITY NOTICE

The authors are the only responsible for the printed material included in this paper.